Annales
Geophysicae

Non-magnetic aspect sensitive auroral echoes from the lower E region observed at 50 MHz

R. Rüster, K. Schlegel

Max-Planck-Institut für Aeronomie, Katlenburg-Lindau, Germany

Abstract. Backscatter from E-region irregularities was observed at aspect angles close to 90° (almost parallel to the direction of the magnetic field) using the ALOMAR SOUSY radar at Andoya/Norway. Strong electric fields and increased E-region electron temperatures simultaneously measured with the incoherent scatter facility EISCAT proved that the Farley-Buneman plasma instability was excited. In addition, strong particle precipitation was present as inferred from EISCAT electron densities indicating that the gradient drift instability may have been active, too. Backscatter at such large aspect angles was not expected and has not been observed before. The characteristics of the observed echoes, however, are in many aspects completely different from usual auroral radar results: the Doppler velocities are only of the order of 10 m/s, the half-width of the spectra is around 5 m/s, the echoes originate at altitudes well below 100 km, and they seem to be not aspect-sensitive with respect to the magnetic field direction. We, therefore, conclude that the corresponding irregularities are not caused by the mentioned instabilities and that other mechanism have to be invoked.

Key words. Ionosphere (plasma waves and instabilities; ionosphere irregularities; particle precipitaion) · Meteorology and atmospheric dynamics (middle atmosphere dynamics)

1 Introduction

Auroral backscatter, i.e. the backscatter from electron density irregularities, created by plasma instabilities in the auroral E region was extensively studied over the past three decades (see Haldoupis, 1989, for a review). Two plasma instabilities, the Farley-Buneman instability (FBI) (Farley, 1963; Buneman, 1963), and the gradient drift instability (GDI) (Simon, 1963) are usually quoted to be responsible for the irregularities. Whereas the FBI needs a threshold electric field of about 15–20 mV/m to be excited, the GDI requires only very small electric fields but in addition sharp electron density gradients.

The irregularities are assumed to be elongated parallel to the direction of the geomagnetic field, since the mobility of the electrons is much larger along the magnetic field lines than perpendicular to $\vec{B}$. The density structures can therefore only be observed if the aspect angle condition, $\vec{k} \cdot \vec{B} = 0°$, is met, where $\vec{k}$ is the wave vector along the radar beam. To fulfill this condition an auroral radar has to be located far south of the scattering region. An aspect angle $\alpha = 0°$ means that this condition is strictly met. Studies of the backscatter at varying aspect angles have shown that the echo intensity decreases very strongly with aspect angles (e.g. André, 1983; Nielsen, 1988). At aspect angles greater than about 5° auroral backscatter can only be recorded by very powerful radars (e.g. Schlegel and Moorcroft, 1989). To our knowledge the observation of auroral backscatter at aspect angles near 90° has never been attempted before.

VHF-radar observations in the mesosphere at high geographic latitudes have been carried out using the ALOMAR SOUSY radar. In summer the radar echoes are known to be very strong. These polar mesospheric summer echoes (PMSE), on average, occur between about 80 and 90 km, centered around 86 km (e.g. review of Cho and Röttger, 1997). Several campaigns using the ALOMAR SOUSY radar have been carried out to investigate the echoing structures and the dynamics associated with them in recent years (e.g. Hoffmann et al., 1995; Rüster, 1995; Bermer et al., 1996; Rüster et al., 1996). The radar-observing programme was specially designed for this purpose and not for the observation of E-region plasma irregularities. We, therefore, were surprised to see echoes occasionally that turned out to be associated with high electric fields as well as with particle precipitation. The present work deals with a typical case of such observations.

In the next section we briefly describe the ALOMAR SOUSY radar. A presentation of the results follows together with measurements from the incoherent scatter facility EISCAT (Baron, 1984) which is located about 120 km east-northeast of the SOUSY radar site. A discussion of the results in terms of the present knowledge of auroral backscatter completes the study.

2 The ALOMAR SOUSY radar

The ALOMAR SOUSY radar (Singer et al., 1995) is identical with the mobile SOUSY radar (Czechowsky et al., 1984), except for the size of the phased antenna array. It is located near the Andoya Rocket Range at Andenes in northern Norway (69° N, 16° E). The radar was operated at a frequency of 53.5 MHz, and detected therefore irregularities of about 3 m scale length. The peak pulse power during the observational period was 150 kW and the duty cycle 4%. The pulses were phase coded using a 16-bit complementary code. The range resolution in the measurements presented here was 300 m. The phased antenna array consisted of 148 four-element Yagis. The side lobes in the E-plane are more than 50 dB below the main lobe at off-zenith directions greater than 60°. The resulting main beam with a one-way-beam width of 6.5° was sequentially steered into five independent positions, vertically (V) and at 8° off-zenith towards north (N), east (E), south (S) and west (W). In each position measurements were made for about 6.6 s such that one cycle lasted 33 s.

3 Results

Overview

Figure 1 presents the observation of 18/19 June 1996 in a concise form. The period in question was moderately disturbed, Kp was 4^-, 4^+, 3 during the last 3-h interval of June 18 and the first two of June 19. The upper part shows in a colour-intensity plot the signal-to-noise ratio (SNR) received by the ALOMAR SOUSY radar with the vertically pointing beam as a function of height and time. The colour scale was adjusted to show clearly the unusual backscatter, the PMSE dominating in the altitude range between about 83 km and 89 km are therefore out of scale. The echoes are visible as vertical structures covering a height range from the upper boundary of the PMSE to the limit of the present observations at 101.3 km.
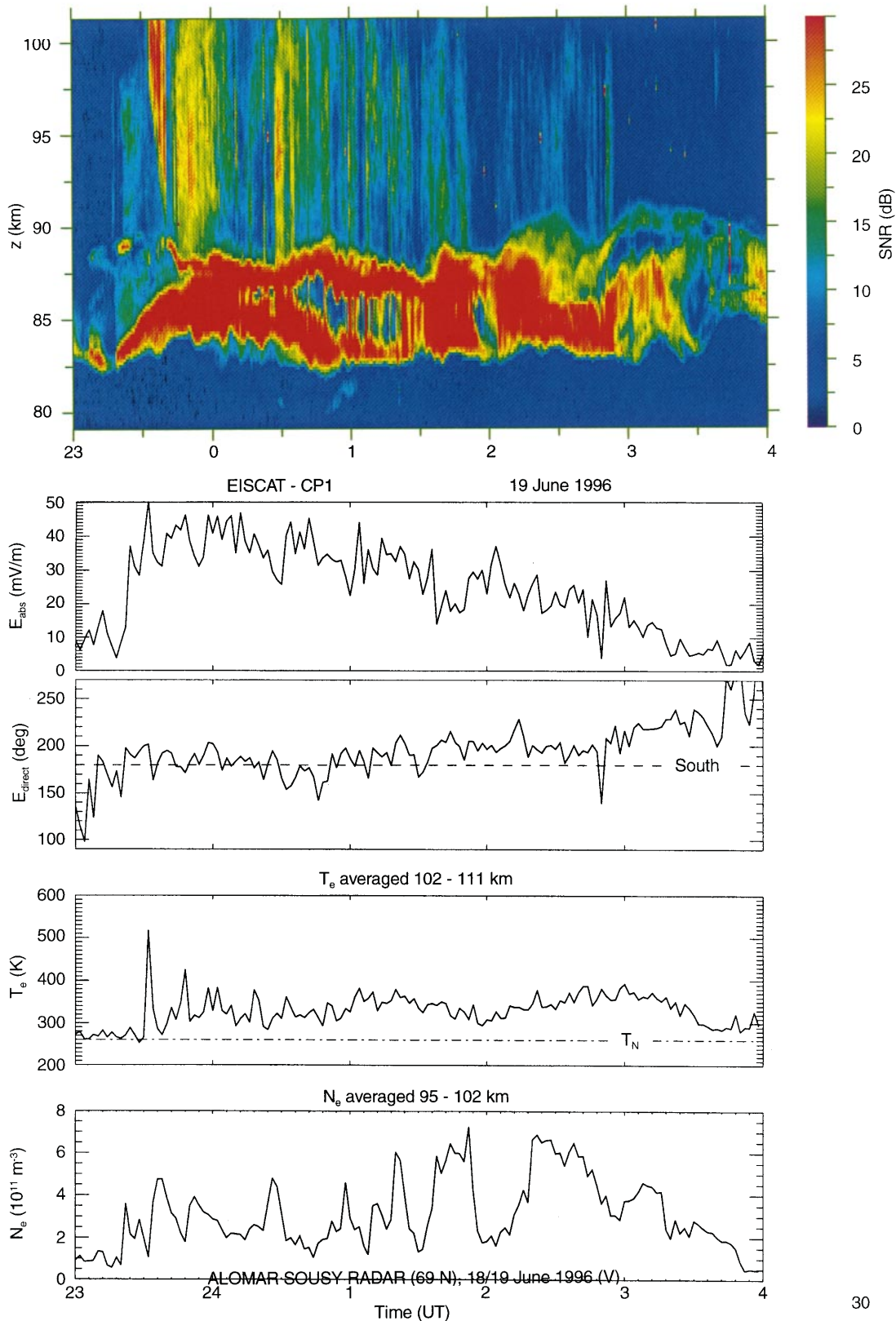
In the second panel the magnitude of the electric field derived from EISCAT tristatic measurements (CP-1) is plotted. A considerable correlation with the echo structure in the uppermost plot is discernible. The backscatter starts at 23:24 UT, approximately at the rise time of the electric field and ends at about 3:00 UT when the electric field drops below about 15 mV/m. This means that the FBI was excited during this time interval.

The direction of the electric field, presented in the third plot, was more or less southward corresponding to the westward electrojet. Regarding the distance between both radars and the drift velocity (≈900 m/s eastwards), a time lag of about 2 min can be expected between the SOUSY and the EISCAT records.

The fourth panel gives another proof that the FBI was excited. The irregularities interact with the ambient electrons thereby enhancing the temperature of the electron gas in a layer between about 100–110 km (Schlegel and St. Maurice, 1981). The electron temperature, shown in this panel, measured by EISCAT was averaged over three height gates from 102–111 km. This averaged electron temperature is enhanced with respect to the neutral temperature T_N from about 23:30 UT until the end of the displayed interval, the peak in T_e clearly corresponds to the peak in the electric field occurring at 23:32 UT. The moderate electron temperature enhancement of about 50–100 K lasting until about 3:30 UT during relatively low electric fields may not only be caused by the FBI but most probably also by particle heating. Energy input by high energy (several keV) particle precipitation occurring after midnight causes an increase of T_e as well as of T_N.

This strong precipitation caused an increase in electron density at low altitudes measured by EISCAT and plotted (as an average over three height gates) in the lowest panel of Fig. 1. A high correlation coefficient of 0.85 ($+0.09/-0.14$ at a 95%-confidence level) between this averaged density and the ALOMAR SOUSY backscattered power (averaged between 98.6 and 101.3 km) was found for the first hour of the displayed interval.
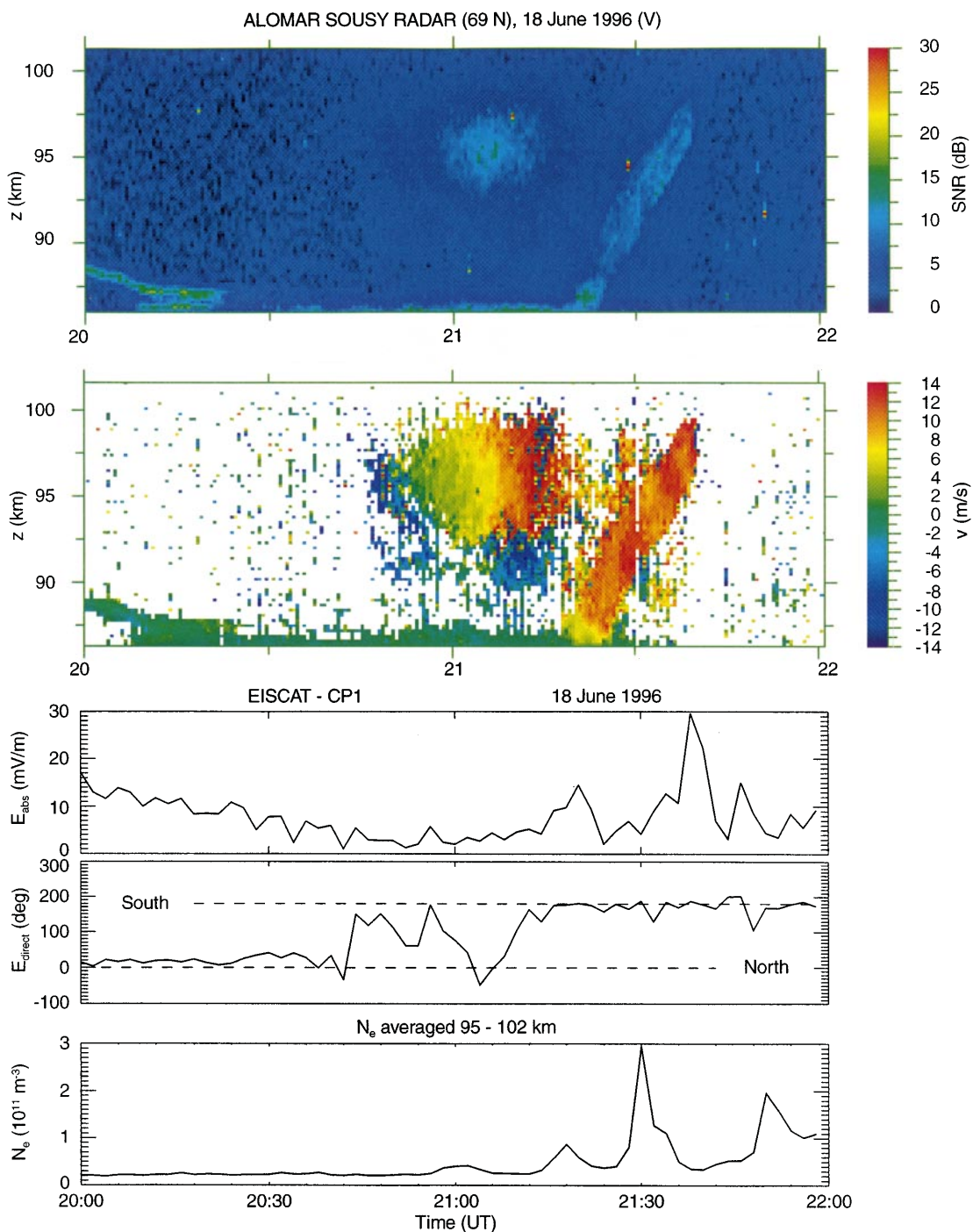
A second interval of backscatter occurring a few hours earlier on the same day was associated with very different conditions (Fig. 2). The colour panel at the top exhibiting the same scale as in Fig. 1 indicates that the power was generally weaker in this case but very distinct in height and time. The upward-slanted trace between 21:20 UT and 21:40 UT is a remarkable feature and in some sense opposite to the downward-moving layer documented in Fig. 3 and discussed below. We have no satisfactory explanation for this behaviour. As second panel we have added a colour presentation of the vertical Doppler velocity during this event. It shows a slow and continuous increase of the velocity from a downward (before about 20:55 UT) to an upward direction. It should be noted that this velocity behaviour is not related straight forward to the electric field change displayed in the third and fourth panel. Contrary to the other event the electric field was weak during this interval and reversed its sign around 21:15 UT according to the change from the evening (westward) to the morning (eastward) convection. This field is certainly too low during the time of backscatter to excite the FBI. The lowest panel reveals that the averaged electron density, as an indication of particle precipitation, is considerably smaller than in the other case. This may explain the weaker backscatter which nevertheless shows some correlation with the averaged density.

Fig. 1. Height-time intensity plot of the signal-to-noise ratio (SNR) observed in the vertically (V) pointing beam with the ALOMAR SOUSY radar at Andenes/Norway (*upper panel*), magnitude and direction (*second and third panel*) of the electric field, electron temperature (*fourth panel*) and electron density (*lowest panel*) averaged over 95 to 102 km. The last four quantities have been derived from EISCAT measurements
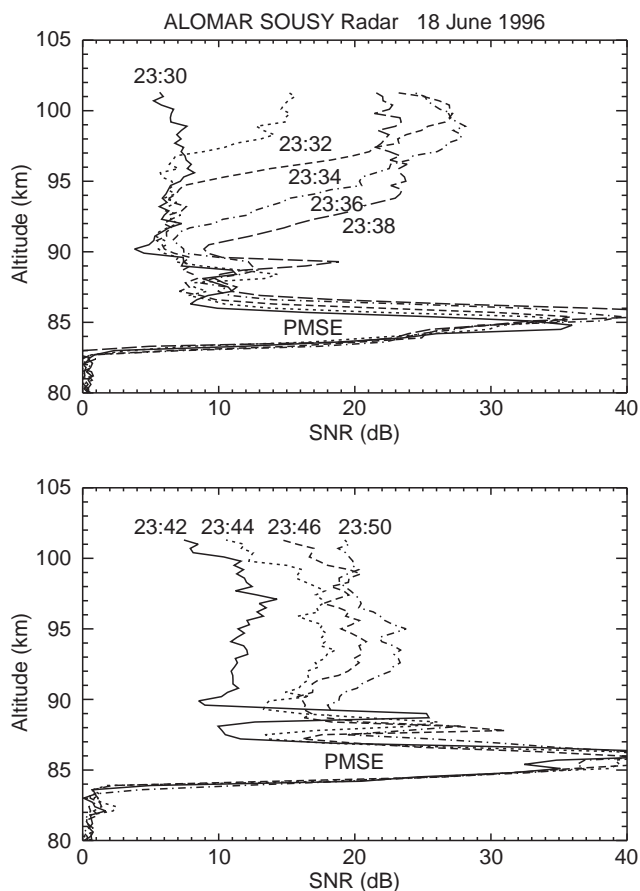
Fig. 2. Similar to Fig. 1, but for a second interval of backscatter occurring earlier on June 18. Electron temperature is omitted in this case, but vertical Doppler velocity of the scatterers (*second panel*) is included

Different beam directions

Since the ALOMAR SOUSY radar observed in five different radar beam directions it was tempting to look at the echoes recorded from directions other than the vertical depicted in Figs. 1 and 2. For this purpose the time interval between 23:30 UT and 23:45 UT during a strong burst of backscatter was examined in more detail. The upper panel of Fig. 5 (the other panels will be explained later) shows the backscattered power in all five beams averaged over 10 height gates, from 98.6 to 101.3 km. The strongest backscatter was recorded in the vertically directed beam, in all other directions it was lower but of comparable magnitude. The observations in the vertically pointing beam, however, do not always show the strongest echoes. The relative power in the different beam directions varies strongly with height and time. During the same time interval but at altitudes around 90 km the strongest echoes were measured in the southward directed beam. Between 0:30 UT and 1:00

Fig. 3. Sequences of height profiles of the signal-to-noise ratio for different time intervals recorded with the vertically pointing beam of the ALOMAR SOUSY radar on June 18, 1996. The saturated echoes of the PMSE are also indicated

UT at altitudes around 90–95 km the strongest scatter was observed in the northward beam, and around 21:10 UT and 90 km height in the eastward beam. This variability seems to indicate that aspect angle effects are not of major importance for the observed phenomenon. Since the magnetic field inclination is about 77° at the SOUSY site, the aspect angle of the N, V, and S beams are $\alpha = 69°$, 77°, 85°, respectively. The different backscatter, therefore, seems to be mainly due to spatial and temporal inhomogeneities in the area where the plasma becomes unstable. At an altitude of 95 km the 8°-angle difference between the beams corresponds to a horizontal distance of 13 km which is large compared to small-scale auroral structures (several 100 m). It can not be assumed, therefore, that the scattering volume is uniform for all beams.

Height profiles

Since usual auroral radars provide no height resolution of the backscattered power, unless interferometer techniques are used (Providakes *et al.*, 1983, 1988), it is interesting to study the 300-m resolution data of the ALOMAR SOUSY radar in more detail. Figure 3 (upper panel) shows five successive height profiles of

the backscattered power. It is evident that the echoing layer moves downward in this case; the fact that it is a layer can be derived from the fact that the two profiles at 23:34 UT and 23:36 UT show a clear maximum at 100 km and 98.5 km, respectively. Later the whole height range between about 93 km and the upper limit of the observations seems to be filled with scatterers.
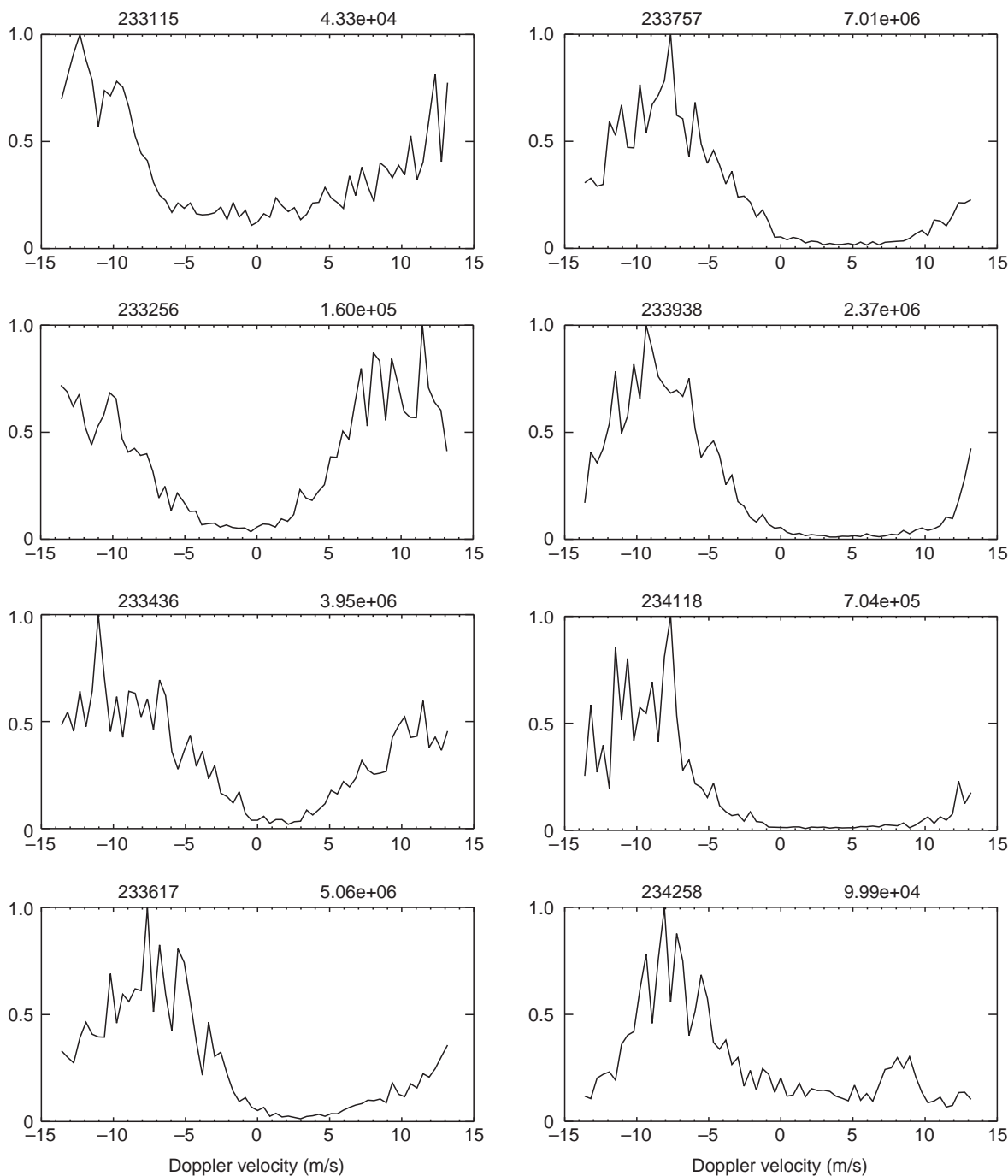
This downward motion may be associated with a hardening of the spectrum of the particles precipitating during this time interval, enabling them to penetrate deeper into the atmosphere. Such a steepening of the auroral particle spectrum is well known from rocket and satellite experiments ('inverted V events', e.g. Hoffman and Lin, 1981).

The scatter profiles recorded about 15 min later (Fig. 3, lower panel) are quite different: A broad maximum of the backscatter develops around 93–95 km from a low level without a descending motion. This behaviour is apparently more common. Similar profile sequences are found after 0:29 UT in many short-lived 'bursts' until 2:55 UT, and also after 21 UT (see Fig. 2). A comparison with the averaged density (Fig. 1, lowest panel) reveals that precipitation was present during all of these bursts.

Shape and moments of spectra

We also examined the spectra of the echoes which were recorded with a height resolution of 300 m and a time resolution of 6.6 s for all five beam positions. The spectra for the time interval from 23:30 to 23:45 UT were averaged between 98.6 and 101.3 km as mentioned before. An additional temporal smoothing over three cycles (99 s) was performed. Fig. 4 shows a sequence of spectra recorded between 23:30 and 23:45 UT using the vertical beam data. At the top of each subplot the end time of the averaging interval and the total backscattered power are given. The spectra cover the frequency range from −4.7 to +4.7 Hz, but the horizontal axis is converted from frequency f to velocity V, according to the Doppler relation $V = (\lambda_r/2)f$, with λ_r being the radar wavelength. Positive velocities are directed upward. The spectra have been normalized to unity in order to see their structure more clearly. Apart from the first two, observed during low backscatter, a relatively stable power distribution at negative velocities develops later. Compared to usual auroral radar spectra (Watermann *et al.*, 1989) they exhibit more structure which is not surprising, regarding the small scattering volume, and their width is considerably smaller. In the first three spectra aliasing is visible, since the mean Doppler velocity is close to the limits of the velocity range.

The corresponding sequence of Doppler velocities and widths are displayed in the lower two panels of Fig. 5 for all five beam directions. Velocities aliased due to the limited frequency range of the spectra have been corrected. (It should be kept in mind that the experiment was designed to measure small, nearly

Fig. 4. Sequence of backscatter spectra recorded with the vertically pointing beam of the ALOMAR SOUSY radar averaged over ten height gates from 98.6–101.3 km. Above each subplot the time and the backscattered power (arbitrary units) are indicated. Negative velocities correspond to a downward motion

vertical velocities of the neutral gas of a few m/s.) Before 23:35 and after 23:44 UT the signal-to-noise ratio is relatively small (see first panel) such that the mean Doppler velocity, derived from the first moment of the spectrum, becomes unreliable. During the period, concerned, however, when the signal-to-noise ratio is large, the velocity is remarkably constant at about 9 m/s. This speaks against aliasing, since a larger variation in the mean velocity would be expected in the case of aliasing. Also the slow and steady velocity variation displayed in

Fig. 2 (second panel) is an indication that the mean Doppler velocity is probably not affected by aliasing during this event.

The half-width of the spectra (third panel of Fig. 5) is generally around 5 m/s. In the case of well-defined spectra during high backscatter (23:35–23:40 UT) the width curves exhibit only a small scatter contrary to the values during lower backscatter power.

We also examined spectra recorded at other time and height intervals (e.g. during the event displayed in
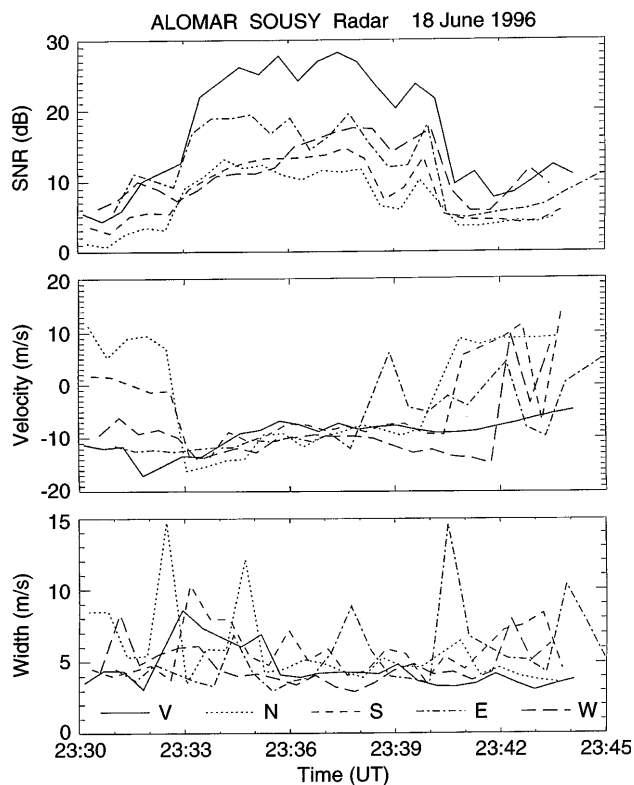
Fig. 5. The first three moments of spectra recorded between 23:30 and 23:45 UT in all five beam direction of the ALOMAR SOUSY radar. The *line styles* corresponding to the different beam directions, indicated in the *lower panel*, apply to all *three panels*

Fig. 2). They all were very similar in shape to those displayed in Fig. 4.

General occurrence

The ALOMAR SOUSY radar operated for about 50 days from May to July 1996. On 12 days during this interval clear echoes of the type described here were detected, on eight additional days weak patches of backscatter were recorded. The event described here was one of the strongest and the only one during which also EISCAT data were available. It is remarkable that very strong geomagnetic disturbances are apparently not required. During five of these 20 mentioned events the magnetic perturbation of the nearby Tromsö magnetometer was below 200 nT, in only three cases above 500 nT. Although the magnetometer data provide only a crude indication of the conditions in the lower ionosphere (they reflect currents, i.e. precipitation and electric fields), these numbers indicate relatively moderate disturbances. A more detailed study of the frequency of occurrence and its relationship to geomagnetic conditions is under way.

4 Discussion

First we want to clarify the term 'backscatter' used throughout this study to characterize the observed phenomenon. This term is used in a very broad sense in the literature for many different scattering mechanisms. We want to stress that it is used here not in the sense of 'auroral backscatter' which is always associated with the two stream or the gradient drift instability within the ionospheric community. We have also considered the possibility that the echoes do not originate from a scattering process, but rather constitute a kind of partial reflection from relatively stable layers, or a mixture of both processes. This would explain the narrow, almost line-type spectra. We did not find, however, any indication of such a layer in the EISCAT data.

Comparing our results to usual auroral backscatter caused by the FBI or GDI, there are at least four surprising details:

Height of the echoes

The height of the maximum backscatter usually is assumed to be in the 100- to 110-km range, as shown by interferometer measurements (see review of Haldoupis, 1989). For most auroral radars, therefore, the aspect angle condition $\alpha = 0°$ is tried to be met at this height. The maximum electron temperature enhancement, related to the irregularity intensity, was also found to be between 105 and 110 km (Schlegel and St.-Maurice, 1981). Our results recorded with a height resolution of 300 m, about an order of magnitude better than interferometer measurements, show that strong backscatter is observed at heights well below 100 km. We certainly cannot rule out that peaks of the scatter profile occur also higher up, because of the limited range in this experiment. It should be noted, however, that rocket measurements have also found relatively intense electron density and electric field fluctuations down to below 90 km (e.g. Pfaff *et al.*, 1987, 1992; Rinnert, 1992; Rose, 1992; Schlegel, 1992). These fluctuations have often been assumed to be associated with the GDI.

Backscattered power

The observed strong backscatter is certainly the most puzzling result, regarding current theories. According to the linear FBI and GDI theory no echoes should be observable at aspect angles greater than a few degrees. A recent experimental study of aspect sensitivities at 50 MHz taking refraction into account, yielded values of about 13 dB/degree at 3°, and 4 dB/degree at 5° (Hall and Moorcroft, 1992). If the latter value is assumed to be valid even down to aspect angles of about 90°, it would be impossible to detect echoes from irregularities nearly parallel to $\vec{B}$.

We can very roughly compare the volume backscatter coefficient for our large aspect angle echoes with those observed at $\alpha \approx 0°$ in the following way. We apply a radar equation suitable for volume backscatter (Farley *et al.*, 1981):

$$P_r = P_t \frac{\eta^2 c\tau \lambda^2 G}{32\pi^2 r^2}\sigma$$

(where P_r, P_t is received and transmitted echo power, η is antenna efficiency, τ is transmitter pulse width, λ is radar wave length, G is receiver antenna gain, r is distance to the scattering volume, and σ is volume backscatter cross section) to two different radars of comparable operating wavelength: our radar and the CUPRI radar of the Cornell group which was widely used for auroral studies (e.g. Providakes et al., 1988, additional information has been provided by J. Sahr, private communication).

Using the data given in Table 1 we obtain a ratio $\sigma(AS)/\sigma(CUPRI)$ of 1/30. This ratio means that the ALOMAR SOUSY radar usually records irregularities with a cross section about 15 dB smaller than that usually observed by CUPRI.

For the sake of completeness it should be mentioned that echoes through antenna side lobes are very unlikely. As already stated in Sect. 2, the antenna used is very insensitive in the direction of the magnetic field normal. Moreover, the scattering volume for such magnetic aspect sensitive echoes would be located about 800 km north of the present observing area. This means that such an excellent correlation with the EISCAT measurements as actually observed, would be very unlikely.

Doppler velocities

Although there are uncertainties with respect to aliasing we can state that during strong backscatter the observed Doppler velocities are very small compared to those usually inferred from auroral radar measurements. Current theories agree in their prediction that Doppler velocities of type 1 spectra should be of the order of the ion acoustic speed (i.e. around 300 m/s) or higher, depending on the magnitude and direction of the electric field. This is confirmed by many experiments. If we assume that a component of the $\vec{E} \times \vec{B}$-drift, being perpendicular to $\vec{B}$, is mapped into directions close to vertical, in which we observe, we should see at least several 10 m/s. We actually observe much lower values.

Gradient drift waves, on the other hand, may exhibit much smaller phase velocities and therefore the corresponding line-of-sight Doppler velocity for our geometry may be in the range of the mean Doppler velocities measured here ($\approx$10 m/s). Two facts, however, speak against these waves in our case: they are confined to

small aspect angles and their spectra are generally much broader (see next section).

Width of the spectra

The width of type 1 spectra, assumed to originate from FBI-induced irregularities, is usually of the order of 100 m/s (Haldoupis, 1989). Only a few examples of very narrow spectra with a width of some 10 m/s have been observed (Providakes et al., 1983). Our measurements show that the spectra during strong backscatter generally exhibit a half-width below 10 m/s. From the point of view of usual auroral radar spectra, they are virtually line spectra. The inverse of the width, the correlation time, can be regarded as a measure of the echo stability. Our echoes, therefore, seem to be considerably more stable than those observed at small aspect angles. The narrow spectra would also not support secondary irregularities (type 2) which are usually much broader than 100 m/s at small aspect angles (Waterman et al., 1989).

The fact that the width is of the same order of magnitude as the mean Doppler velocity seems to point towards a cascading process, typical for secondary gradient drift waves. But it is known from theory (Sudan, 1983) that this cascading would not markedly change the orientation of the scatterers with respect to the magnetic field, i.e. they would be observable only at small aspect angles.

It is obvious from the four items discussed that the observed echoes are most probably not caused by the FBI. The apparent coincidence of high electric fields and the backscatter displayed in Fig. 1 are not causally related. During disturbed conditions high electric fields are always present at the edges of auroral arcs which, in turn, are related to particle precipitation. The magnitude of the electric field observed during one of our events is sufficient to excite the FBI, but the irregularities which we observe can hardly be caused by this instability, as outlined. The small electric fields prevailing during the other event (Fig. 2) are evidence against the FBI as the cause of backscatter, too. Similarly we can rule out the GDI. Both instabilities cannot be regarded separately, they are described by a common dispersion relation and the irregularities are field-aligned in both cases. The confinement of the echoes to low aspect angles, therefore, also applies to the GDI.

Particle precipitation on the other hand seems to be clearly related to the observed backscatter. From the electron densities in the height range of 90–100 km derived from EISCAT observations, it can be concluded that precipitation must have been present during the intervals of backscatter documented here. During the other events mentioned in Sect. 3 (not discussed in detail here) particle precipitation was very likely, too.

Particle precipitation, on the other hand, may not necessarily be related to the generation mechanism. Since the backscattered power is proportional to the square of the electron density fluctuations, particle precipitation may just enhance but not create them. This question is subject of another study (Robinson and Schlegel, 1999).

Table 1. Operating parameters for two different 50-MHz radars

Radar - parameters	ALOMAR SOUSY	CUPRI
Frequency	53.5 MHz	46.9 MHz
Transmitter power	150 kW	20 kW
Receiver antenna gain	29 dB	14 dB
Range to scattering volume	95 km	600 km
Pulse length	2 μs	50 μs
Typical signal-to-noise ratio	25 dB	15 dB

5 Summary and conclusions

Our results show that very strong echoes from auroral irregularities can be observed nearly parallel to the magnetic field. The backscatter sometimes occurs simultaneously with high electric fields, but it is always associated with particle precipitation. The echoes are, on average, 10–15 dB weaker than those usually observed by a typical 50-MHz auroral radar (CUPRI) at perpendicular incidence. Further unexpected results are the strong echo power down to 90 km altitude, the low Doppler velocities, and the very narrow shape of the spectra.

To our knowledge none of the current theories can explain all the observed features. Our purpose was to document and to describe this new backscatter phenomenon, a thorough theoretical explanation is beyond its scope. Further studies, particularly from the theoretical point of view, are necessary to understand and to interpret our results. One possible explanation is discussed in an accompanying study (Robinson and Schlegel, 1999, submitted).

References

André, D., The dependence of the relative backscatter cross section of 1m-density fluctuations in the auroral electrojet on the angle between electron drift and the radar wave vector, *J. Geophys. Res.*, **88,** 8043–8049, 1983.

Baron, M., The EISCAT facility, *J. Atmos. Terr. Phys.*, **46,** 469–472, 1984.

Bremer, J., P. Hoffmann, W. Singer, C. E. Meek, and R. Rüster, Simultaneous PMSE observations with ALOMAR-SOUSY and EISCAT-VHF radar during the ECHO-94 campaign. *Geophys. Res. Lett.*, **23,** 1075–1078, 1996.

Buneman, O., Excitation of field aligned sound waves by electron streams, *Phys. Rev. Lett.*, **10,** 285–287, 1963.

Cho, J. Y. N., and J. Röttger, An updated review of polar mesosphere summer echoes: observation, theory, and their relationship to noctilucent clouds and subvisible aerosols, *J. Geophys. Res.*, **102,** 2001–2020, 1997.

Czechowsky, P., G. Schmidt, and R. Rüster, The mobile SOUSY Doppler radar: technical design and first results, *Radio Sci.*, **19,** 441–450,1984.

Farley, D. T., A plasma instability resulting in field-aligned irregularities in the ionosphere, *J. Geophys. Res.*, **68,** 6083–6097, 1963.

Farley, D. T., H. M. Ierkic, and B. G. Fejer, The absolute scattering cross section at 50 MHz of equatorial electrojet irregularities, *J. Geophys. Res.*, **86,** 1569–1575, 1981.

Haldoupis, C., A review on radio studies of auroral E-region ionospheric irregularities, *Ann. Geophysicae* **7,** 239–258, 1989.

Hall, G., and D. R. Moorcroft, Magnetic aspect angle effects in radar aurora at 48.5 MHz, corrected for refraction, *J. Geophys. Res.*, **97,** 19471–19488, 1992.

Hoffman, R. A., and C. S. Lin, Study of inverted-V auroral precipitation events, in *Physics of auroral arc formation*, Eds. S.-I. Akasofu and J. R. Kan American Geophysical Union, Washington, D.C., USA, 1981, pp 80–90.

Hoffmann, P., J. Bremer, W. Singer, R. Rüster, and A. H. Manson, PMSE Observations with the ALOMAR SOUSY Radar and the EISCAT VHF radar during summer 1994, *Proc. of the 12th ESA Symp.*, *Lillehammer*, ESA sp-370, 73–79, 1995.

Nielsen, E., Aspect angle dependence of backscatter intensity of 1-m auroral plasma waves, *J. Geophys. Res.*, **93,** 4119–4124, 1988.

Pfaff, R. F., M. C. Kelley, E. Kudeki, B. G. Fejer, and K. D. Baker, Electric field and plasma density measurements in the strongly driven daytime equatorial electrojet, 1. The unstable layer and gradient drift waves, *J. Geophys. Res.*, **92,** 13,578–13,596, 1987.

Pfaff, R. F., J. Sahr, J. F. Providakes, W. E. Swartz, D. T. Farley, P. M. Kintner, I. Häggström, A. Hedberg, H. Opgenoorth, G. Holmgren, A. McNamara, D. Wallis, B. Whalen, A. Yau, S. Watanabe, F. Creutzberg, P. Williams, E. Nielsen, K. Schlegel and T. R. Robinson, The E-region rocket radar instability study (ERRIS): scientific objectives and compaign overview, *J. Atmos. Terr. Phys.*, **54,** 779–808, 1992.

Providakes, J., D. T. Farley, B. G. Fejer, J. Sahr, W. E. Swartz, I. Häggström, A. Hedberg, and J. A. Nordling, Observations of auroral E-region plasma waves and electron heating with EISCAT and a VHF radar interferometer, *J. Atmos. Terr. Phys.*, **50,** 339–356, 1988.

Providakes, J. F., W. E. Swartz, D. T. Farley, and B. G. Fejer, First VHF auroral radar interferometer observations, *Geophys. Res. Lett.*, **10,** 401–404, 1983.

Rinnert, K., Plasma waves observed in the auroral E-region – ROSE campaign, *J. Atmos. Terr. Phys.*, **54,** 683–692, 1992.

Rose, G., Three component a.c. E-field observations during the rocket and scatter experiment in 1988–1989 under radar auroral conditions in northern Scandinavia. *J. Atmos. Terr. Phys.*, **54,** 669–682, 1992.

Rüster, R., Velocity and associated echo power variations in the summer polar mesosphere, *Geophys. Res. Lett.*, **22,** 65–67, 1995.

Rüster, R., P. Czechowsky, P. Hoffmann and W. Singer, Gravity wave signatures at mesopause heights, *Ann. Geophysicae.*, **14,** 1186–1191, 1996.

Schlegel, K., Measurements of electron density fluctuations during the ROSE rocket flights, *J. Atmos. Terr. Phys.*, **54,** 715–724, 1992.

Schlegel, K., and J. P. St.-Maurice, Anomalous heating of the polar E region by unstable plasma waves, I. Observations, *J. Geophys. Res.*, **86,** 1447–1452, 1981.

Schlegel, K., and D. R. Moorcroft, EISCAT as an auroral radar, *J. Geophys. Res.*, **94,** 1430–1438, 1989.

Simon, A., Instability of a partly ionized plasma in crossed electric and magnetic fields, *Phys. Fluids*, **6,** 382–388, 1963.

Singer, W., D. Keuer, P. Hoffmann, P. Czechowsky, and G. Schmidt, The ALOMAR SOUSY radar: technical design and further developments, *Proc. of the 12th ESA Symp.*, *Lillehammer*, ESA sp-370, 409–415, 1995.

Sudan, R. N., Unified theory of type I and type II irregularities in the auroral electrojet, *J. Geophys. Res.*, **88,** 4853–4860, 1983.

Watermann, J., A. G. McNamara, G. J. Sofko, and J. A. Koehler, Distribution of mean Doppler shift, spectral width, and skewness of coherent 50-MHz auroral radar backscatter. *J. Geophys. Res.*, **94,** 6979–6985, 1989.